Cysteine Labeling Studies Detect Conformational Changes in Region 106−132 of the Mitochondrial ADP/ATP Carrier of *Saccharomyces cerevisiae*†

Yoshitaka Kihira,‡ Eiji Majima,‡,# Yasuo Shinohara,‡,§,⊥ and Hiroshi Terada*,‡,||

Faculty of Pharmaceutical Sciences, University of Tokushima, Shomachi-1, Tokushima 770-8505, Japan, APRO Life Science Institute, Inc., Muyacho, Naruto 772-0001, Japan, Institute for Genome Research, University of Tokushima, Kuramotocho-3, Tokushima 770-8503, Japan, Single-Molecule Bioanalysis Laboratory, National Institute of Advanced Industrial Science and Technology (AIST), Hayashicho 2217-14, Takamatsu 761-0395, Japan, and Faculty of Pharmaceutical Sciences, Tokyo University of Science, Noda-shi Yamazaki 2641, Chiba 278-8510, Japan

Received June 2, 2004; Revised Manuscript Received October 19, 2004

ABSTRACT: To know the structural and functional features of the cytosolic-facing first loop (LC1) including its surrounding region of the mitochondrial ADP/ATP carrier (AAC), we prepared 27 mutants, in which each amino acid residue between residues 106 and 132 of the yeast type 2 AAC (yAAC2) was replaced by a cysteine residue. For mutant preparation, we used a Cys-less AAC mutant, in which all four intrinsic cysteine residues were substituted with alanine residues, as a template [Hatanaka, T., Kihira, Y., Shinohara, Y., Majima, E., and Terada, H. (2001) *Biochem. Biophys. Res. Commun. 286*, 936−942]. From the labeling intensities of the membrane-impermeable SH-reagent eosin-5-maleimide (EMA), sequence Lys^{108}−Phe^{127} was suggested to constitute the LC1. The N-terminal half of this region (Lys^{108}−Phe^{115}) was suggested to change its location from the cytosol to a region close to the membrane on conversion from the c-state to the m-state in association with disruption or unwinding of its alpha-helical structure, whereas the C-terminal half region (Gly^{116}−Phe^{127}) was considered to extrude essentially into the cytosol, while keeping its alpha-helical structure. Hence, the conformation of m-state LC1 is greatly different from that of c-state LC1. Possibly the LC1 changes its location between the membranous region and the cytosol during ADP/ATP transport. Lys^{108} in the LC1 of the yAAC2 was found to be associated with binding of the transport substrates, and its $-NH_3^+$ moiety, to be of importance for the transport function. On the basis of these results, possible roles of the conformational changes of the LC1 in the transport activity are discussed.

The ADP/ATP carrier (AAC),[1] a member of the mitochondrial solute carrier family, in the mitochondrial inner membrane exports ATP synthesized by oxidative phosphorylation into the cytosol in concert with the import of ADP into the matrix (*1*−*3*). This carrier consists of about 300 amino acid residues, and they form a tandem repeat structure of three homologous domains, each of which contains about 100 amino acid residues. The AAC shows two distinct conformations known as the c-state and m-state, in which the nucleotide-binding site faces the cytosol and matrix, respectively (*3*−*6*). Transport of ADP/ATP is achieved by interconversion between these conformations (*4*, *7*). The irreversible transport inhibitor carboxyatractyloside (CATR) and the reversible inhibitor atractyloside (ATR) fix the carrier in the c-state conformation, whereas bongkrekic acid (BKA) fixes it in the m-state conformation (*4*, *5*). From studies on hydrodynamic (*8*), cross-linking (*9*, *10*), inhibitor binding stoichiometry (*11*, *12*), and electrophoresis (*13*, *14*), it has long been thought that AAC functions as a dimer. In addition, the transport function of the tandem repeated homodimer of the yeast type 2 AAC (yAAC2), in which the carboxyl terminus of the first repeat is linked to the amino terminus of the second repeat, was found to be very similar to that of the native yAAC2, suggesting that these N- and C-termini in the dimeric form of AACs are located on the same side of the membrane (*15*).

Recently, the crystal structures of the c-state yeast type 3 AAC fixed by ATR (*16*) and c-state bovine type 1 AAC fixed by CATR were reported (*17*). The crystal structure of the bovine type 1 AAC clearly showed six transmembrane segments, each consisting of an alpha-helix, and there were three loops on the matrix side (LM1 to LM3), and two loops (LC1 and LC2) and N- and C-termini on the cytosolic side (see Figure 1). These features are essentially the same as those predicted previously from the results of site-directed mutagenesis and chemical modification studies (*18*, *19*). These crystal structures suggest that the transport is achieved

† This work was supported by grants-in-aid for scientific research from the Ministry of Education, Science and Culture of Japan (14370746 to Y.S.).

* Correspondence author: Faculty of Pharmaceutical Sciences, Tokyo University of Science, Yamazaki 2641, Noda, Chiba 278-8510, Japan. Fax: +81-04-7121-3663, E-mail: teradah@rs.noda.tus.ac.jp.

‡ Faculty of Pharmaceutical Sciences, University of Tokushima.

APRO Life Science Institute, Inc.

§ Institute for Genome Research, University of Tokushima.

⊥ National Institute of Advanced Industrial Science and Technology (AIST).

|| Tokyo University of Science.

[1] Abbreviations: AAC, ADP/ATP carrier; yAAC2, yeast type 2 AAC; CATR, carboxyatractyloside; BKA, bongkrekic acid; EMA, eosin-5-maleimide; MTS, methanethiosulfonate; MTSEA, 2-aminoethyl MTS; MTSES, 2-sulfonatoethyl MTS; MTSET, 2-(trimethylammonium)ethyl MTS; PAGE, polyacrylamide gel electrophoresis; DTT, dithiothreitol; SDS, sodium dodecyl sulfate.

10.1021/bi0488653 CCC: $30.25
Published on Web 12/04/2004

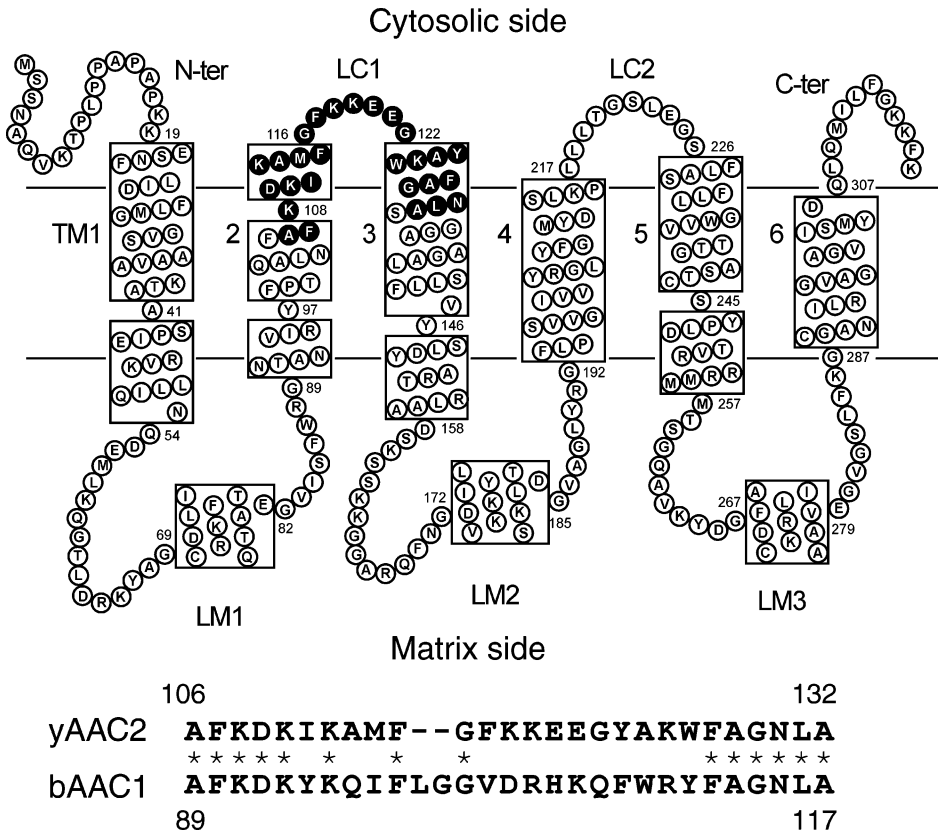

FIGURE 1: Possible topology of amino acid residues of the c-state yAAC2 in the mitochondrial inner membrane. The possible 6-transmembrane alpha-helical span model of yAAC2 is constructed according to the results of crystal structure of the c-state bovine type 1 AAC (*17*). Boxes represent alpha-helices, and the residues mutated to cysteine residue in this study are shown by solid circles. In the model, the first and second loop facing the cytosol and first, second, and third loops facing matrix are shown by LC1, LC2, LM1, LM2, and LM2, respectively. The alignments of the peptide sequence of bovine and yeast carrier are shown under the illustration. In these alignments, amino acid residues conserved in both carriers are marked with asterisks (∗). (All residues are shown by bold letters.)

via its monomer unit, although the carrier seems to form a dimer in the membrane (*8*−*14*). However, detailed structures associated with transport function should further be studied.

From our earlier studies on chemical modification with SH-reagents, we showed that the loops facing the matrix were decisively important for the transport-associated recognition and binding of the transport substrates ATP and ADP (*18*, *20*−*23*). A large extent of translocation of the LM1, which functions as a gate for the transport, from the membrane to the matrix takes place upon induction of the m-state from the c-state, and such a large extent of change in LM1 characterizes these conformational states of the AAC (*10*, *20*, *23*). In addition, the region around Cys^{159} in the LM2 of the bovine type 1 carrier is thought to function as a major recognition site of substrates from the matrix side (*21*, *22*).

Although the roles of loops facing the matrix in the transport process are well characterized, little is known about the loops facing the cytosol (LC1 and LC2) or the N- and C-terminus regions. In a previous study, we constructed cysteine-less (Cys-less) yAAC2, in which all four intrinsic cysteine residues were substituted with alanine residues (*19*). The Cys-less yAAC2 was found to show essentially the same functional properties as the wild-type yAAC2. Furthermore, by using Cys-less yAAC2 as a template, we succeeded in preparing various yAAC2 mutants, in which amino acid residues of the yAAC2 were substituted with cysteine residues (*19*).

In the present study, we sought to characterize the LC1, which is a linking region on cytosolic surface between the second and third transmembrane segments, of the yAAC2. Using Cys-less yAAC2 as a template, we constructed a series of mutants, in which each of amino acid residues 106−132 was substituted with a cysteine, and examined their reactivities toward the SH-reagents eosine-5-maleimide (EMA) and methanethiosulfonate (MTS) derivatives. On the basis of the different reactivities of these cysteine residues in the LC1 and its surrounding region, we discussed the structural and functional features of this loop.

EXPERIMENTAL PROCEDURES

Materials. The haploid strain of *Saccharomyces cerevisiae* W303-1B (MATα *ade2-1 leu2-3,112 his3-22,15 trp1-1 ura3-1 can1-100*) (*24*) was obtained from Dr. Shimizu (Osaka University). The AAC-disrupted strain of WB-12 (MATα *ade2-1 leu2-3,112 his3-22,15 trp1-1 ura3-1 can1-100 aac1::LEU2 aac2::HIS3*) and the yeast shuttle vector pRS314-YA2P were prepared as described earlier (*25*). [^{14}C]-ADP was obtained from DuPont-New England Nuclear (Wilmington, DE); CATR, from Sigma (St. Louis); and EMA, from Molecular Probes (Eugene). Methanethiosulfonate (MTS) reagents, i.e., 2-aminoethyl MTS (MTSEA), 2-sulfonatoethyl MTS (MTSES), and 2-(trimethylammonium)-ethyl MTS (MTSET), were purchased from Toronto Research Chemicals (Toronto). BKA was a gift from Prof. Duine (Delft University of Technology). Other materials and reagents were of the highest grade commercially available.

Mutagenesis. Mutant carriers were generated by site-directed mutagenesis of the Cys-less yAAC2, in which all

four cysteine residues had been replaced by alanine residues (*19*). All of the mutations were confirmed by DNA sequencing. The DNA fragments prepared were subcloned into pRS314-YA2P for transformation of the AAC-disrupted yeast strain, as described previously (*25*). Yeast cells were grown at 30 °C in YP medium consisting of 1% yeast extract and 2% bactopeptone supplemented with either 2% glucose (YPD), 2% galactose (YPGal), or 3% glycerol (YPGly) as a carbon source. For selection of transformants, the cells were grown at 30 °C in SD medium consisting of 0.67% yeast nitrogen base w/o amino acids and 2% glucose supplemented with standard concentrations of nutritional requirements when necessary (*26*). Solid media contained 2% Bacto-Agar (Difco Laboratories) (*25*).

Detection of AAC. Yeast mitochondria were isolated, as described previously (*25*). For detecting the AAC in mitochondria, we subjected mitochondrial proteins to SDS−PAGE and Western blot analysis using antiserum against a synthetic peptide (Ser^2−Ser^{21}) of the yAAC2-specific sequence (*25*). The amount of AAC in mitochondria was determined by use of an ATTO model AE-6900 image analyzer from the intensity of the immunostained band in terms of the amount of yAAC2 (*25*).

Labeling with SH-Reagents EMA and MTS. For EMA-labeling, yeast mitochondria (8 mg of protein/mL) were first pretreated with 100 μM BKA, CATR, or ATR for 30 min at pH 7.4 and 25 °C, and then the samples diluted with ST medium (250 mM sucrose, 10 mM Tris-HCl buffer, pH 7.4) to 4 mg of protein/mL were incubated with 200 μM EMA for 30 min at pH 7.4 and 0 °C in the dark. After subsequent labeling was terminated with 10 mM DTT at pH 7.4 and 25 °C for 5 min, the labeled samples were subjected to SDS−PAGE on 15% polyacrylamide gels in the dark, and the degree of EMA labeling was determined by measuring the fluorescence intensities of the stained bands by means of the ATTO model AE-6900 image analyzer. For analyzing the EMA-labeling of proteins modified with MTS-reagents, mitochondria pretreated with MTS-reagents in STE medium (250 mM sucrose, 0.2 mM EDTA-2Na, 10 mM Tris-HCl buffer, pH 7.4) in the presence of oligomycin were centrifuged, and the supernatant was removed. The mitochondria were solubilized by incubation with 1% SDS in 25 mM Tris-HCl (pH 7.4) for 5 min and then incubated with 200 μM EMA for 30 min at pH 7.4 and 0 °C in the dark. The labeled samples were immediately subjected to SDS−PAGE under nonreducing conditions. For labeling with MTS-reagents, mitochondria (1 mg of protein/mL) suspended in STE medium containing 1 μg/mL oligomycin were treated with 2.5 mM MTSEA, 1 mM MTSET, or 10 mM MTSES for 5 min at 0 °C.

ADP Transport Activity. ADP transport activity of yeast mitochondria was determined essentially as described previously (*27*). Mitochondria (1 mg of protein/mL) suspended in STE medium with 1 μg/mL oligomycin were stood for 5 min at 0 °C, and then 100 μM [^{14}C]ADP (specific radioactivity, 37 kBq/μmol) was added. After incubation of the sample for various periods at 0 °C, ADP uptake was terminated with 20 μM CATR and 5 μM BKA. The amount of [^{14}C]ADP incorporated was determined from its radioactivity in an Aloka LSC-3500 liquid scintillation counter. The initial rate of ADP transport was determined as described previously (*28*).

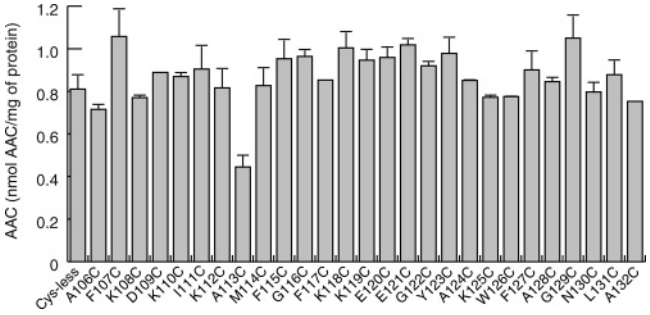

FIGURE 2: Expression levels of single cysteine mutants of the ADP/ATP carrier of the yAAC2 determined by Western blotting. Proteins of the isolated mitochondria transformants, in which single cysteine mutants were expressed, were subjected to SDS−PAGE and Western blotting analysis using antibodies raised against the yAAC2-specific sequence (Ser^2 to Ser^{21}). The intensities of the immunostained band were measured with an ATTO model AE-6900 image analyzer.

RESULTS

Construction and Characterization of Single-Cysteine Mutants. Our previous study showed that cysteine residues are not essential for the transport function of the yeast type 2 ADP/ATP carrier (yAAC2), because Cys-less yAAC2, in which all cysteine residues were substituted with alanine residues, showed ADP transport activity similar to that of the wild-type yAAC2 (*19*). Thus, to understand structural and functional features of this loop, we prepared a series of mutants in which each of amino acid residues 106−132 in the first loop facing cytosol (LC1) and its surrounding region of the yAAC2 was separately substituted with a cysteine residue. The possible topology of yAAC2 in light of the crystal structure of the bovine AAC, and amino acid residues of the LC1 and its surrounding region are summarized in Figure 1. Each of these single cysteine mutants was expressed in the AAC-disrupted yeast strain WB-12, in which the intrinsic type 1 and type 2 AACs had been disrupted (*25*).

In 5 days, all transformants grew to levels similar to the level of the Cys-less transformant on plates with fermentable glucose as a carbon source. When nonfermentable glycerol was used as a carbon source, most of the single cysteine transformants grew like the Cys-less transformant during the 5 days; however, the A113C transformant did not grow even after 7 days, and the growth of the transformants Y123C, K125C, and F127C was as low as approximately 50% of that of the Cys-less transformant.

The mitochondrial proteins isolated from each yeast transformant cultivated with fermentable galactose were subjected to SDS−PAGE, and the AAC expressed in single cysteine mutants was detected by Western blotting using specific yAAC2 antiserum against the amino terminus region (Ser^2−Ser^{21}) of yAAC2. As shown in Figure 2, all AAC mutants except A113C were expressed in the mitochondria to an extent similar to that of the parental Cys-less yAAC2. In contrast, the expression level of A113C was as low as approximately 50% of that of the others.

The initial velocities of ADP uptake of the mitochondria of transformants were next determined at pH 7.4 and 0 °C. As shown in Figure 3, transport activities of almost all mutants were in a range between 40 and 100% of the activity of the Cys-less yAAC2, whereas those of A113C, Y123C, K125C, and F127C were only 2−15% of it, thus suggesting

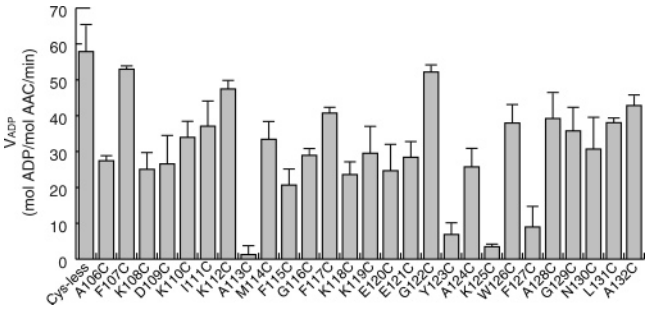

FIGURE 3: ADP transport activities of single cysteine mutants of the yAAC2. Isolated mitochondria (1 mg of protein/mL) of transformants of yAAC2 were suspended in medium containing 1 μg/mL oligomycin, and then 100 μM [^{14}C]ADP (specific radioactivity, 37 kBq/μmol) was added. After incubation of the sample for various periods at 0 °C, ADP uptake was terminated with 20 μM CATR and 5 μM BKA. The amount of [^{14}C]ADP incorporated was determined from its radioactivity in an Aloka LSC-3500 liquid scintillation counter, and the initial rate of ADP transport was determined by the method described previously (*28*). Values are means ± SD in three runs.

that Ala^{113}, Tyr^{123}, Lys^{125}, and Phe^{127} are important for the transport activity.

Reactivities of Cysteine Mutants with EMA. We next examined the effect of the fluorescent SH-reagent eosin-5-maleimide (EMA) on the cysteine residues of mutants. For this, mitochondria expressing each single cysteine mutant were pretreated with 100 μM BKA or CATR to fix the carrier in the m- and c-state conformation, respectively, and then were treated with 200 μM EMA for 30 min at pH 7.4 and 0 °C in the dark. EMA labeled the yAAC2 of almost all of the single cysteine mutants. To confirm that the mitochondrial membrane is not permeable to EMA, we prepared the C73-mutant, in which all four cysteine residues except Cys^{73} located on the matrix side were substituted by alanine residues (*19*), and then examined its reactivity with EMA. EMA labeled neither the Cys^{73} of the C73-mutant nor the Cys-less mutant (Figure 4), showing that EMA is a membrane-impermeable SH-reagent, as we suggested previously (*18*, *19*), and that EMA modifies cysteine residues exposed to the cytosol. We also confirmed that EMA labeled the phosphate carrier (PiC) (*19*). The results of SDS−PAGE of EMA-treated mitochondria pretreated with CATR or BKA are shown in Figure 4.

Figure 5 shows the fluorescence intensities due to EMA-labeling of c- and m-state carriers. Location of cysteine residues of the cysteine mutants in the mitochondrial membrane can be estimated from their reactivities to EMA based on the assumption that the EMA-labeling is dependent on the degree of exposure of cysteine residues to the cytosol. This assumption was supported by the results showing that the fluorescence intensities due to EMA-labeling were dependent on the cysteine mutants, whereas those of all mutants showed almost the same high fluorescence intensities by EMA-labeling after denaturation of the mutants with 1% SDS (data not shown).

The results showing that the single cysteine mutants A106C, F107C, A128C, G129C, L131C, and A132C were not modified with EMA in either the m- or c-state suggest that Ala^{106}, Phe^{107}, Ala^{128}, Gly^{129}, Leu^{131}, and Ala^{132} are intruded into the mitochondrial membrane. Hence, the sequence Lys^{108}−Phe^{127} should be located in an aqueous environment, such as the cytosol. We referred to the sequence Lys^{108}−Phe^{127} as LC1. Alignment of amino acid residues of the LC1 and its surrounding regions in the yeast carrier, and their EMA-labeling intensities in the c-state conformation are shown in Figure 6, in light of the crystal structure of the bovine carrier (*17*).

In the bovine carrier, the corresponding sequence constitutes an extended region between the second and third transmembrane alpha-helices (Figures 1 and 6) (*17*). As N130C of yAAC2 was labeled to some extent in both conformational states, Asn^{130} at the cytosolic end of the third transmembrane helix should be located close to the membrane surface in the interhelical gap in such a way that its side chain is extended toward the aqueous transport pore, like the corresponding Asn^{115} of the bovine carrier (Figure 6) (*17*). It is noteworthy that EMA labeled G116C−F127C mutants in such a way that the labeling was essentially independent of the conformational state. Hence, the region comprising Gly^{116}−Phe^{127} is suggested to be located in a similar position regardless of the two conformational states of the carrier. Hereafter, we refer to this region as the C-terminal half of LC1, the location of which is insensitive to the conformational state of the carrier. EMA-labeling intensities of these mutants showed a periodic pattern with lower labeling intensities of E120C, A124C, and F127C interspersed among higher ones, possibly because the region Gly^{116}−Phe^{127} forms essentially an alpha helix, and Glu^{120}, Ala^{124}, and Phe^{127} are located at a position, to which the polar anionic EMA has difficulty in gaining access, such as at the aqueous/membrane interface. A wheel model of the sequence Gly^{116}−Phe^{127} showed that residues having low EMA-labeling intensities are located on one side, with EMA-accessible ones on the other side (Figure 7A), suggesting that this region consists of an alpha-helix. In contrast, the crystal structure of c-state bovine AAC shows that the corresponding region consists of an alpha-helix and random coil, as shown in Figure 6 (*17*).

The fluorescence intensities of the region Lys^{108}−Phe^{115}, which we refer to as the N-terminal half of LC1, were greatly dependent on the conversion between m-state and c-state (Figure 5). In the c-state conformation, the labeling intensities of the N-terminal half were higher for the mutants D109C and K112C, and the intensities of the two or three residues after each of these residues decreased in a stepwise fashion. Such changes in the labeling intensities suggest that this region forms an alpha-helix in the c-state. In fact, the wheel model of the N-terminal half shows that the residues with high fluorescence intensity of EMA and those with poor EMA-labeling are located on different sides (Figure 7B). Hence, the N-terminal half could form an alpha-helix like the corresponding region of the CATR-bound bovine carrier (Figures 1 and 6) (*17*).

In contrast, labeling intensities of amino acid residues in the N-terminal half in the m-state carrier were very similar except in the case of K108C, and they were in general lower than those of the c-state carrier. This low EMA-labeling should not be due to any inhibitory effect of the bound BKA, but due to the conformational change resulting from the conversion to the m-state carrier, because the binding site of BKA is located in the second loop facing matrix (LM2), to which BKA gains access from the matrix side after crossing the mitochondrial membrane (*4*, *21*). In addition,

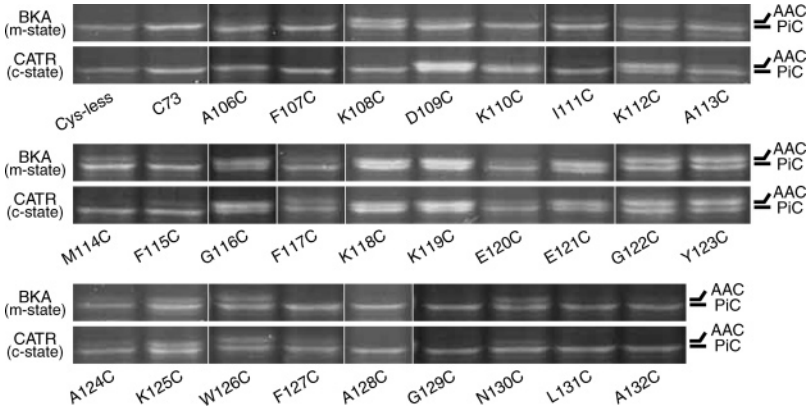

FIGURE 4: EMA-labeling of single cysteine mutants of yAAC2. Mitochondria, in which each mutant was expressed, were incubated with either 100 μM BKA or CATR for 30 min at 25 °C, and then incubated with 200 μM EMA for 30 min at pH 7.4 and 0 °C in the dark. The protein samples were subjected to SDS−PAGE on 15% polyacrylamide gels in the dark. After electrophoresis, EMA-labeling was detected from the fluorescence due to the labeling. AAC, yAAC2; PiC, phosphate carrier; C73, the mutant in which all the intrinsic cysteine residues except Cys^{73}, located in the LM1, were replaced with alanine residues.

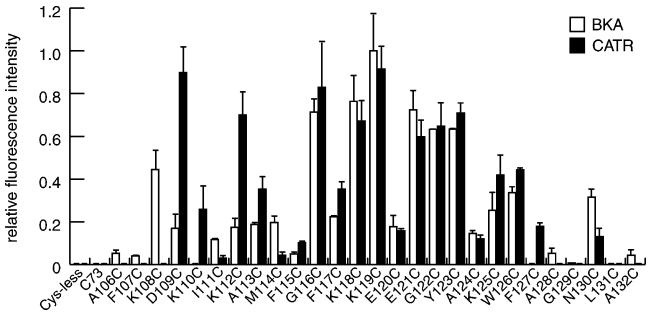

FIGURE 5: Labeling intensities of single cysteine mutants of the ADP/ATP carrier labeled with EMA. Fluorescence intensities due to EMA-labeling of single cysteine mutants of the yAAC2 shown in Figure 4 were determined in an ATTO model AE-6900 image analyzer. Then the intensities were expressed in terms of the amount the corresponding single cysteine mutant shown in Figure 2. The corrected fluorescence intensities relative to that of K119C treated with BKA, which showed the greatest intensity, are shown. Open and closed columns represent the mitochondria treated with BKA and CATR, respectively. C73, the mutant in which all the intrinsic cysteine residues except Cys^{73}, located in the LM1, were replaced with alanine residues. Results are means ± SD of at least three runs.

if BKA binds to (a) certain residue(s), EMA-labeling intensities should be residue-dependent. However, labeling intensities in the m-state were similar for all residues of the N-terminal half of LC1, as shown in Figures 4 and 5. The concentration of BKA used (100 μM) is much greater than its IC_{50} of 10 μM (*21*), and is adequate for complete inhibition of EMA-labeling (*21*). Hence, the N-terminal half is suggested to change its conformation according to the conformational state of the carrier. It is possible that the alpha-helical N-terminal half is located in the polar environment such as in the cytosol in the c-state, whereas it is transferred to a region that EMA accesses with difficulty, such as in the membrane or close to the membrane surface, on conversion to the m-state due to a change in the alpha-helical conformation.

In addition, the significantly low labeling of K108C fixed in the c-state by the irreversible inhibitor CATR might be due to the possibility that Lys^{108} is associated with the binding of CATR, as in the case for the corresponding Lys^{91} of the bovine type 1 AAC (*17*). If so, EMA could not label CATR-bound K108C. For confirming this possibility, we examined EMA-labeling of K108C in the c-state induced by ATR. As binding of ATR is reversible, being competitive with EMA, it would be expected that EMA could attack K108C by displacing the bound ATR. In fact, EMA-labeling of the carrier fixed in the c-state by the reversible inhibitor ATR was significantly greater than that in the m-state, as shown in Figure 8. Hence, both EMA and CATR are highly accessible to c-state K108C.

Effects of Introduction of Charged Groups onto the Cysteine Residue of Single Cysteine Mutants. There are nine charged residues, i.e., Lys^{108}, Asp^{109}, Lys^{110}, Lys^{112}, Lys^{118}, Lys^{119}, Glu^{120}, Glu^{121} and Lys^{125}, in the LC1 loop. To know the roles of these charged residues in the transport, we next examined the effects of labeling with methanethiosulfonate (MTS) derivatives on ADP transport of K108C, D109C, K110C, K112C, K118C, K119C, E120C, E121C, and K125C. For this, we used the cationic 2-aminoethyl MTS (MTSEA), cationic 2-(trimethylammonium)ethyl MTS (MTSET), and anionic 2-sulfonatoethyl MTS (MTSES) to introduce a cationic or anionic charge (see Chart 1). These reagents attack cysteine residues of proteins (P) and form disulfide adducts P-S-SCH_2CH_2X, in which X stands for NH_3^+ (MTSEA), $N(CH_3)_3^+$ (MTSET), or SO_3^- (MTSES). Thus, a positive or negative charge can be introduced to a cysteine residue (*29*, *30*).

We treated isolated yeast mitochondria with MTS-reagents for 5 min at pH 7.4 and 0 °C, solubilized mitochondria with 1% SDS, and then treated them with 200 μM EMA for 30 min at 0 °C in the dark. Then, mitochondrial proteins were subjected to SDS−PAGE. EMA did not further label cysteine residues of these MTS-treated mutants, showing that the MTS-reagents had completely labeled cysteine residues of these single cysteine mutants. Then, we determined the amount of ADP taken up by mitochondria after incubation of mitochondria with 100 μM [^{14}C]ADP at pH 7.4 and 0 °C for 5 min, as a measure of transport activity.

Figure 9 shows the amount of ADP transported in 5 min via the AAC of MTS-labeled single cysteine mutant relative to that of each mutant without treatment with MTS-reagents. As ADP transport activity of the Cys-less mutant was not affected by labeling with MTS-reagents at all, MTS-labeling of mitochondrial proteins other than the AAC did not affect the ADP transport. Hence, the effects of MTS-labeling of

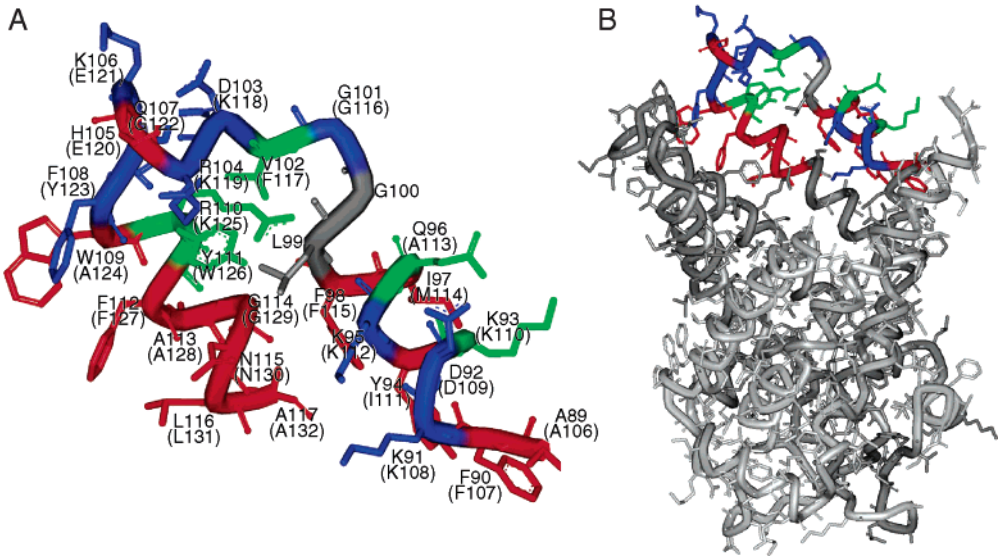

FIGURE 6: Possible alignment of amino acid residues and their EMA-labeling intensities in the LC1 and its adjacent regions of the c-state yAAC2. In A, alignment of the amino acid sequence of the region between Ala[106] and Ala[132] in the yeast AAC, which is equivalent to residues between Ala[89] and Ala[117]of the bovine AAC, is depicted in light of the crystal structure of the c-state bovine AAC (*17*). The residue number is that of the bovine carrier, and that of the yeast carrier is shown in parentheses. The residues without a corresponding yeast sequence number are because the sequence of the bovine carrier of this region is two residues longer than that of the yeast carrier. The residues in blue, green, and red represent those with relative EMA-labeling intensities that were high, intermediate, and low, according to the scores of 1.0−0.6, 0.6−0.2 and 0.2−0, respectively, shown in Figure 5. As the corresponding residues of Leu[99] and Glu[100] of the bovine carrier are lacking in the yeast carrier, these residues are shown as gray ones. In B, the c-state structure of the entire AAC is shown. The bovine structure was downloaded from the Protein Data Bank (http://www.rcsb.org/pdb/) and depicted with a Viewer Lite 50.

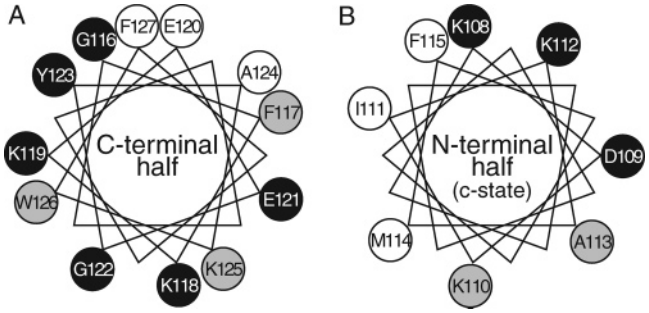

FIGURE 7: Helical arrangement of amino acid residues of C-terminal half (A) and N-terminal half (B) of the LC1 loop. Helical arrangement is shown according to the wheel model. Amino acid residues labeled with EMA significantly (intensities 1.0−0.6 in Figure 5), intermediately (0.6−0.2), and quite weakly (0.2−0) are shown by solid, gray, and open circles, respectively.

single cysteine mutants were regarded to be due solely to introduction of cationic or anionic charges.

MTS affected significantly the ADP transport of K108C and K112C, but it did not affect that of the other mutants. Namely, the uptake was considerably increased by labeling of K108C with the cationic MTSEA and was decreased significantly by labeling with the anionic MTSES. Labeling with the cationic MTSET also increased the uptake, but less than that with MTSEA. In addition, introduction of the negative charge to Cys[112] of K112C by modification with MTSES decreased greatly ADP uptake, whereas introduction of either of the positive charges to this mutant did not affect the transport activity.

To examine the importance of the positive charge of residue 108 in more detail, we prepared the mutants K108R and K108D, and determined the initial transport rate of ADP transport. As summarized in Table 1, the transport activity decreased in the order of MTSEA-labeled K108C > Cys-less mutant > K108R > K108C > MTSES-labeled K108C

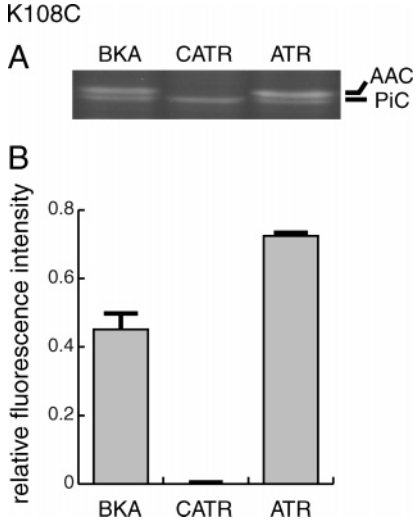

FIGURE 8: EMA-labeling of the mutant K108C treated with various transport inhibitors. Mitochondria of K108C transformant were incubated with 100 μM BKA, CATR, or ATR for 30 min at 25 °C, and then incubated with 200 μM EMA for 30 min at pH 7.4 and 0 °C in the dark. Mitochondrial protein samples were subjected to SDS−PAGE on 15% polyacrylamide gels in the dark. (A) Results of SDS−PAGE; (B) intensities due to the yAAC2 labeled with EMA, in which values are the means ± SD of at least three runs. AAC, yAAC2; PiC, phosphate carrier.

= K108D, showing the importance of positive charge at this position. Here again, the negative charge was shown to be unfavorable for ADP transport. We next determined the kinetic parameters of ADP transport for the Cys-less mutant, K108C, and MTSEA-labeled K108C. As summarized in Table 2, the V_{max} values were almost the same for these mutants, but the K_m values for ADP were different in the order of MTSEA-labeled K108C > Cys-less > K108C. Hence, MTSEA-labeling of Cys[108] increased the affinity of Lys[108] in the Cys-less mutant for ADP, and abolishment of

Chart 1. Structures of the Methanethiosulfonate (MTS) Derivatives Used in this Study[a]

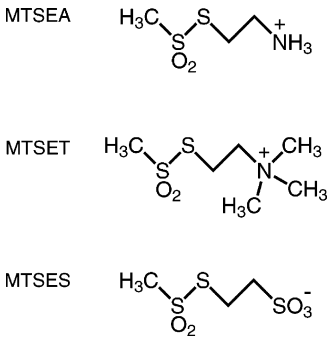

[a] MTSEA, MTSET, and MTSES represent 2-aminoethyl MTS, 2-(trimethylammonium)ethyl MTS, and 2-sulfonatoethyl MTS, respectively.

the positive charge of residue 108 decreased the affinity for ADP.

DISCUSSION

There are six membrane spanning regions along with three loops facing the matrix (LM1, LM2, and LM3), two loops facing the cytosol (LC1 and LC2), and amino and carboxyl termini both facing the cytosol in the ADP/ATP carrier (Figure 1). Although the loops facing the matrix have already been well characterized, little is known about those facing the cytosol. To understand some of the features of the cytosolic surface of the AAC, we characterized in this study the structural and functional properties of the LC1 of the yeast type 2 ADP/ATP carrier (yAAC2).

We constructed single cysteine mutants, in which each residue between residue 106 and residue 132 was replaced with a cysteine residue, by using Cys-less yAAC2 as a template. Almost all the transformants grew like the Cys-less transformant in medium containing glycerol as a nonfermentable carbon source, but the growth of Y123C, K125C, and F127C transformants was about half of that of the Cys-less transformant. Also, the A113C transformant showed no growth at all. As expression of the AAC of the A113C transformant was about 50% of that of the Cys-less AAC, Ala^{113}, which is not conserved in the bovine carrier, could be associated with sorting into the mitochondria and insertion into mitochondrial membrane of the carrier. In addition, most of the mutants showed ADP transport activities ranging between 40 and 100% of the activity of the parental Cys-less yAAC2. However, the transport activities of A113C, Y123C, K125C, and F127C, the growth of which were quite low on nonfermentable carbon source, were significantly lower than that of Cys-less yAAC2, showing that Ala^{113}, Tyr^{123}, Lys^{125}, and Phe^{127} are residues important for the transport activity of the carrier. The bulky residues Tyr^{123}, Lys^{125}, and Phe^{127} located close to the cytosolic end of the third transmembrane segment are likely to be associated with the stabilization of the adjacent membrane spanning helix, as in the corresponding bovine residues in light of the crystal structure of the c-state bovine carrier (Figure 6B) (*17*).

From the reactivity of the residues toward EMA, we found that EMA was accessible to the residues Lys^{108}−Phe^{127}. Hence, we referred to this region as LC1, which could be characterized by two distinct regions comprising N- and C-terminal halves. EMA-labeling of cysteine residues corresponding to Gly^{116}−Phe^{127} (C-terminal half region) was essentially independent of the conformational state of the carrier, and the labeling intensities differed every three or four residues. Namely, EMA-labeling intensities of residues 120, 124, and 127 were low, and the labeling intensity of two or three residues following each of these residues was high, suggesting that this region forms an alpha-helix. The wheel-model of the alpha-helical structure of the C-terminal half showed that residues with low EMA-labeling intensities, such as Glu^{120}, Ala^{124}, and Phe^{127}, are located on the same side of the alpha-helix, and those with high (Glu^{116}, Lys^{118}, Lys^{119}, Glu^{121}, Gly^{122} and Tyr^{123}) and intermediate (Phe^{117}, Lys^{125}, and Trp^{126}) intensities reside on the other side. The highly and intermediately labeled residues should be located in a polar environment, such as the cytosol, whereas the poorly labeled residues are likely to be occluded from reacting with the polar anionic EMA by being located close to the membrane surface. It is noteworthy that yeast Glu^{120} seems to be located close to the membrane in light of the low EMA-labeling, whereas the corresponding bovine His^{105} is fully exposed, possibly due to differences in residue and length of this region. In addition, the positively charged residues Lys^{118}, Lys^{119}, and Lys^{125} are located closely together. This arrangement may be effective for transport activity of the carrier by attracting the polyvalent negatively charged transport substrates ADP/ATP.

In contrast, EMA-labeling of residues Lys^{108}−Phe^{115}, referred to as the N-terminal half region of the LC1, was dependent on the conformational state of the AAC, being greater in the c-state than in the m-state. The labeling intensities of these residues in the c-state carrier varied according to the residue as in the C-terminal half. The helical wheel representation showed that the residues are aligned in such a way that the more highly labeled residues are located on the same surface, whereas the weakly labeled residues are situated on the other surface. Possibly, the N-terminal half of the c-state carrier forms an alpha-helix. In contrast, EMA-labeling intensities of the m-state carrier were quite different from those of the c-state carrier. Upon conversion to the m-state, the N-terminal half might be transferred from the polar cytosol to a region close to the membrane, in which the N-terminal half is occluded not to be labeled with EMA, by disruption or unwinding of the alpha-helical structure, because EMA-labeling intensities of amino acid residues in the N-terminal half of the m-state carrier were almost the same and in general lower than those of the c-state carrier.

It is noteworthy that EMA labeled K108C quite highly in the m-state, but did not label it at all in the c-state. The crystal structure of the c-state bovine type 1 AAC fixed by CATR showed that the corresponding Lys^{91} is involved in binding with CATR (*17*). The lack of EMA-labeling of c-state K108C could thus be due to tightly bound CATR. In fact, the labeling of K108C in the c-state fixed by the reversible inhibitor ATR was increased to a level greater than that in the m-state. Hence, Lys^{108} could be exposed greatly in the c-state as in the m-state. As this residue is located next to the cytosolic terminal end of the second membrane spanning helix, this residue should be of importance for regulating the transport activity of the carrier. Asp^{109} and Lys^{112} located closely together with Lys^{108} would also be expected to take part in this regulation (Figure 6A). These three ionic residues

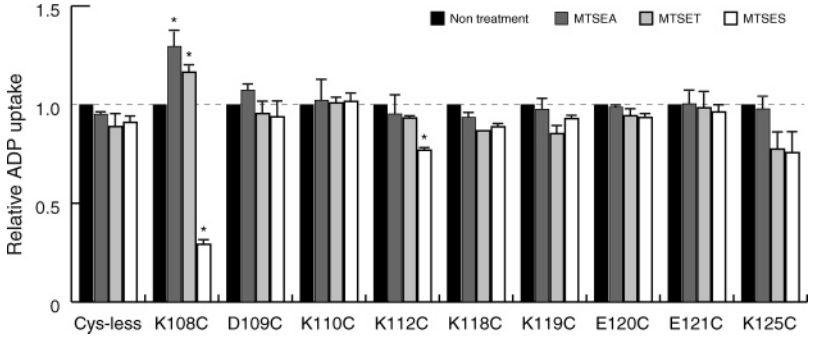

FIGURE 9: Effects of MTS-reagents on ADP uptake of single cysteine mutants. Isolated mitochondria of transformants of single cysteine mutant (1 mg of protein/ml) were pretreated with MTS-reagents for 5 min at 0 °C, and then incubated with 100 μM [^{14}C]ADP for 5 min at 0 °C. Total amounts of ADP incorporated relative to the expressed amount of the corresponding mutant without treatment with MTS-reagents are shown. Values are means ± SD in three or four runs. Asterisks indicate statistically significant differences at the level of $p < 0.01$.

Table 1: ADP Transport Activities of the Mutants K108R and K108D[a]

mutants	V_{ADP} (nmol ADP/ nmol AAC/min)[b]
Cys-less mutant	57.9 ± 7.9
K108R mutant	53.6 ± 3.5
K108D mutant	10.7 ± 1.4
K108C mutant	19.3 ± 3.7
K108C mutant labeled with MTSEA	68.1 ± 2.9
K108C mutant labeled with MTSET	n.d.[c]
K108C mutant labeled with MTSES	10.8 ± 2.4

[a] Isolated mitochondria (1 mg of protein/mL) of transformants of the Cys-less, K108R, K108D, and K108C mutants were suspended in STE medium containing 1 μg/mL oligomycin, and then labeled with 2.5 mM MTSEA, 1 mM MTSET, or 10 mM MTSES for 5 min at 0 °C. ADP uptake was started by incubation of the isolated mitochondria with 100 μM [^{14}C]ADP (specific radioactivity, 37 kBq/μmol) for various periods at 0 °C, and terminated with 20 μM CATR and 5 μM BKA (*28*). [b] Values are means ± SD in at least three separate runs. [c] Not determined.

Table 2: Effect of MTSEA-labeling on the Kinetics of ADP Transport via the AAC of K108C Mutant[a]

	K_m (mM)	V_{max} (mol ADP/ mol AAC/min)
Cys-less mutant	0.20	142.9
K108C mutant without MTSEA-labeling	0.40	116.3
K108C mutant labeled with MTSEA	0.09	140.9

[a] Isolated mitochondria of Cys-less and K108C mutants were incubated in STE containing 1 μg/mL oligomycin for 5 min at 0 °C, and then incubated with various concentrations of [^{14}C]ADP between 10 and 200 μM for various periods at 0 °C. MTSEA-labeling was performed by incubation of the mitochondria of K108C mutant with 2.5 mM MTSEA for 5 min at 0 °C in STE containing 1 μg/mL oligomycin, and then the kinetics of ADP transport was determined. Results are means from at least three separate runs.

seem to be exposed to the cytosol in the c-state, contrary to the corresponding residues of the bovine carrier, which were shown to be located inside of the pore formed by the helical bundle (*17*). In conclusion, the N-terminal half of the c-state carrier is suggested to be located essentially in an aqueous environment, such as the cytosol, taking an alpha-helical conformation, whereas it is transferred to the membrane or close to the membrane, accompanied by disruption or unwinding of alpha-helical structure on conversion to the m-state conformation. Such a ligand-induced large extent of conformational change was reported for the calcium pump, the alpha-helical conformation of which is unwound on interaction with the divalent cationic calcium (*31*). As this conformational change should be caused by reorganization of salt bridges on access of calcium ions, it is possible that the conformational change in the N-terminal half of the LC1 is triggered by binding of the multivalent anionic transport substrates ADP/ATP with their possible binding site Lys^{108}. Hence, this region could act as a gate for the transport activity.

Labeling of K108C and K112C with MTS-reagents showed that a negative charge at residues 108 and 112 was quite unfavorable for transport activity of the carrier. It is interesting to note that the positive charge of residue 108 caused increased transport activity, whereas that at residue 112 did not. In the experiments on the ADP uptake of the K108C mutant labeled with MTSEA$^+$ and the mutants in which Lys^{108} of the Cys-less mutant was replaced by various residues, the transport activity changed in the order of MTSEA$^+$-Cys > Lys$^+$ > Arg$^+$. This order does not represent the order of the molecular size of MTSEA$^+$-Cys (125 Å^3) > Arg$^+$ (122 Å^3) > Lys$^+$(106 Å^3) (*29*). As MTSET$^+$-Cys (173 Å^3), which is a larger cationic moiety than MTSEA$^+$-Cys, failed to increase ADP transport above that of the MTSEA$^+$-modified K108C, the cationic -NH_3^+ moiety is of great importance and independent of the molecular size of the residue. It is noteworthy that Lys$^+$ is more favorable for transport activity than Arg$^+$ as an endogenous cationic amino acid residue, suggesting that Lys^{108} and also Lys^{125} are functionally important, being located in the cytosolic entrance of the transport path. This could be a reason these two Lys residues are conserved in all the AACs, the sequences of which have been determined (*3*).

Previously, we found that LM1, the first loop facing the matrix, acts as a gate in the transport of ADP/ATP from the matrix to the cytosol, to let transport substrates be transferred from the matrix to their primary recognition/binding site in the LM2 by translocation of the extruded LM1 to the membrane. Such a large extent of translocation of LM1 is tightly associated with conversion of the carrier from the m-state to the c-state (*20*). In this study, we found that a similar wide range of translocation of the N-terminal half of the first loop facing the cytosol (LC1) takes place from the cytosol to the membrane surface upon conversion from the c-state to m-state by disruption or unwinding of its alpha-helical structure. This translocation is responsible for conversion of the c-state to the m-state conformation induced by

binding of cytosolic ADP and ATP to the carrier and subsequent their transport to the matrix. Hence, the LC1 could be a swinging gate for the transport of ADP from the cytosol to matrix, like the LM1 in the reversed transport of ATP.

This is the first report of a systematic study on the structural and functional features of the cytosolic surface of the ADP/ATP carrier. Our results showed that the C-terminal half of LC1 of the c-state yAAC2, the structural feature of which is essentially the same as that of the c-state bovine carrier, does not undergo a conformational change on conversion to the m-state. However, the N-terminal half of the LC1 is translocated from cytosol to a position close to the membrane on conversion of the c-state carrier to the m-state. Hence, a similar translocation could take place with the bovine carrier, the m-state conformation of which has not yet been reported. As the LC1 is suggested to act as a gate for the transport by changing its location upon access of the transport substrates, it is possible that the ADP and ATP are essentially transported according to our cooperating swinging loop model, in which the transport is achieved by cooperative translocation of loops facing the matrix and cytosol (*20*).

REFERENCES

1. Pedersen, P. L. (1993) An introduction to the mitochondrial anion carrier family, *J. Bioenerg. Biomembr. 25*, 431−434.
2. Kaplan, R. S. (2001) Structure and function of mitochondrial anion transport proteins, *J. Membr. Biol. 179*, 165−183.
3. Brandolin, G., Le Saux, A., Trezeguet, V., Lauquin, G. J., and Vignais, P. V. (1993) Chemical, immunological, enzymatic, and genetic approaches to studying the arrangement of the peptide chain of the ADP/ATP carrier in the mitochondrial membrane, *J. Bioenerg. Biomemebr. 25*, 459−472.
4. Klingenberg, M. (1989) Molecular aspects of the adenine nucleotide carrier from mitochondria, *Arch. Biochem. Biophys. 270*, 1−14.
5. Klingenberg, M. (1993) Dialectics in carrier research: the ADP/ATP carrier and the uncoupling protein, *J. Bioenerg. Biomembr. 25*, 447−457.
6. Klingenberg, M. (1976) The ADP-ATP carrier in mitochondrial membranes. *The Enzymes of Biological Transport*, Martonosi, A. N., Ed., Vol. 3, pp 383−438.
7. Walker, J. E. (1992) The mitochondrial transporter family, *Curr. Opin. Struct. Biol. 2*, 519−526.
8. Hackenberg, H., and Klingenberg, M. (1980) Molecular weight and hydrodynamic parameters of the adenosine 5′-diphosphate-adenosine 5′-triphosphate carrier in Triton X-100, *Biochemistry 19*, 548−555.
9. Klingenberg, M., Hackenberg, H., Eisenreich, G., and Mayer, I. (1979) The interaction of detergents with the ADP,ATP carrier from mitochondria. *Function and Molecular Aspects of Biomembrane Transport*, Quagliariello, E., Palmieri, F., Papa, S., and Klingenberg, M., Eds., Elsevier, Amsterdam, pp 291−303.
10. Majima, E., Ikawa, K., Takeda, M., Hashimoto, M., Shinohara, Y., and Terada, H. (1995) Translocation of loops regulates transport activity of mitochondrial ADP/ATP carrier deduced from formation of a specific intermolecular disulfide bridge catalyzed by copper-*o*-phenanthroline, *J. Biol. Chem. 270*, 29548−29554.
11. Riccio, P., Aquila, H., and Klingenberg, M. (1975) Purification of the carboxy-atractylate binding protein from mitochondria, *FEBS Lett. 56*, 133−138.
12. Klingenberg, M., Riccio, P., and Aquila, H. (1978) Isolation of the ADP, ATP carrier as the carboxyatractylate-protein complex from mitochondria, *Biochim. Biophys. Acta 503*, 193−210.
13. Palmisano, A., Zara, V., Honlinger, A., Vozza, A., Dekker, P. J., Pfanner, N., and Palmieri, F. (1998) Targeting and assembly of the oxoglutarate carrier: general principles for biogenesis of carrier proteins of the mitochondrial inner membrane, *Biochem. J. 333*, 151−158.
14. Ryan, M. T., Müller, H., and Pfanner, N. (1999) Functional staging of ADP/ATP carrier translocation across the outer mitochondrial membrane, *J. Biol. Chem. 274*, 20619−20627.
15. Hatanaka, T., Hashimoto, M., Majima, E., Shinohara, Y., and Terada, H. (1999) Functional expression of the tandem-repeated homodimer of the mitochondrial ADP/ATP carrier in *Saccharomyces cerevisiae*, *Biochem. Biophys. Res. Commun. 262*, 726−730.
16. Kunji, E. R., and Harding, M. (2003) Projection structure of the atractyloside-inhibited mitochondrial ADP/ATP carrier of *Saccharomyces cerevisiae*, *J. Biol. Chem. 278*, 36985−36988.
17. Pebay-Peyroula, E., Dahout-Gonzalez, C., Kahn, R., Trezeguet, V., Lauquin, G. J., and Brandolin, G. (2003) Structure of mitochondrial ADP/ATP carrier in complex with carboxyatractyloside, *Nature 426*, 39−44.
18. Majima, E., Koike, H., Hong, Y.-M., Shinohara, Y., and Terada, H. (1993) Characterization of cysteine residues of mitochondrial ADP/ATP carrier with the SH-reagents eosin 5-maleimide and *N*-ethylmaleimide, *J. Biol. Chem. 268*, 22181−22187.
19. Hatanaka, T., Kihira, Y., Shinohara, Y., Majima, E., and Terada, H. (2001) Characterization of loops of the yeast mitochondrial ADP/ATP carrier facing the cytosol by site-directed mutagenesis, *Biochem. Biophys. Res. Commun. 286*, 936−942.
20. Terada, H., and Majima, E. (1997) Important role of loops in the transport activity of the mitochondrial ADP/ATP carrier, *Prog. Colloid Polym. Sci. 106*, 192−197.
21. Majima, E., Shinohara, Y., Yamaguchi, N., Hong, Y.-M., and Terada, H. (1994) Importance of loops of mitochondrial ADP/ATP carrier for its transport activity deduced from reactivities of its cysteine residues with the sulfhydryl reagent eosin-5-maleimide, *Biochemistry 33*, 9530−9536.
22. Majima, E., Yamaguchi, N., Chuman, H., Shinohara, Y., Ishida, M., Goto, S., and Terada, H. (1998) Binding of the fluorescein derivative eosin Y to the mitochondrial ADP/ATP carrier: Characterization of the adenine nucleotide binding site, *Biochemistry 37*, 424−432.
23. Hashimoto, M., Majima, E., Goto, S., Shinohara, Y., and Terada, H. (1999) Fluctuation of the first loop facing the matrix of the mitochondrial ADP/ATP carrier deduced from intermolecular cross-linking of Cys56 residues by bifunctional dimaleimides, *Biochemistry 38*, 1050−1056.
24. Lawson, J. E., and Douglas, M. G. (1988) Separate genes encode functionally equivalent ADP/ATP carrier proteins in *Saccharomyces cerevisiae*. Isolation and analysis of AAC2, *J. Biol. Chem. 263*, 14812−14818.
25. Hashimoto, M., Shinohara, Y., Majima, E., Hatanaka, T., Yamazaki, N., and Terada, H. (1999) Expression of the bovine heart mitochondrial ADP/ATP carrier in yeast mitochondria: significantly enhanced expression by replacement of the N-terminal region of the bovine carrier by the corresponding regions of the yeast carrier, *Biochim. Biophys. Acta 1409*, 113−124.
26. Treco, D. A., and Lundblad, V. (1993) *Current Protocols in Molecular Biology*, John Wiley, New York, Chapter 13.1.
27. Nelson, D. R., Felix, C. M., and Swanson, J. M. (1998) Highly conserved charge-pair networks in the mitochondrial carrier family, *J. Mol. Biol. 277*, 285−308.
28. Krämer, R., and Klingenberg, M. (1977) Reconstitution of adenine nucleotide transport with purified ADP, ATP-carrier protein, *FEBS Lett. 82*, 363−367.
29. Akabas, M. H., Stauffer, D. A., Xu, M., and Karlin, A. (1992) Acetylcholine receptor channel structure probed in cysteine-substitution mutants, *Science 258*, 307−310.
30. Xu, Y., Kakhniashvili, D. A., Gremse, D. V., Wood, D. O., Mayor, J. A., Walters, D. E., and Kaplan, R. S. (2000) The yeast mitochondrial citrate transport protein. Probing the roles of cysteines, Arg(181), and Arg(189) in transporter function, *J. Biol. Chem. 275*, 7117−7124.
31. Toyoshima, C., and Nomura, H. (2002) Structural changes in the calcium pump accompanying the dissociation of calcium, *Nature 418*, 605−611.

BI0488653